Biochimica et Biophysica Acta 1833 (2013) 672–679

Contents lists available at SciVerse ScienceDirect

Biochimica et Biophysica Acta

journal homepage: www.elsevier.com/locate/bbamcr

UCP2 inhibition triggers ROS-dependent nuclear translocation of GAPDH and autophagic cell death in pancreatic adenocarcinoma cells

Ilaria Dando, Claudia Fiorini, Elisa Dalla Pozza, Chiara Padroni, Chiara Costanzo, Marta Palmieri, Massimo Donadelli *

Department of Life and Reproduction Sciences, Biochemistry Section, University of Verona, Verona, Italy

ARTICLE INFO

Article history:
Received 17 July 2012
Received in revised form 19 October 2012
Accepted 25 October 2012
Available online 2 November 2012

Keywords:
UCP2
Autophagy
ROS
GAPDH
Cancer
Genipin

ABSTRACT

Mitochondrial uncoupling protein 2 (UCP2) can moderate oxidative stress by favoring the influx of protons into the mitochondrial matrix, thus reducing electron leakage from respiratory chain and mitochondrial superoxide production. Here, we demonstrate that UCP2 inhibition by genipin or UCP2 siRNA strongly increases reactive oxygen species (ROS) production inhibiting pancreatic adenocarcinoma cell growth. We also show that UCP2 inhibition triggers ROS-dependent nuclear translocation of the glycolytic enzyme glyceraldehyde 3-phosphate dehydrogenase (GAPDH), formation of autophagosomes, and the expression of the autophagy marker LC3-II. Consistently, UCP2 over-expression significantly reduces basal autophagy confirming the anti-autophagic role of UCP2. Furthermore, we demonstrate that autophagy induced by UCP2 inhibition determines a ROS-dependent cell death, as indicated by the apoptosis decrease in the presence of the autophagy inhibitors chloroquine (CQ) or 3-methyladenine (3-MA), or the radical scavenger NAC. Intriguingly, the autophagy induced by genipin is able to potentiate the autophagic cell death triggered by gemcitabine, the standard chemotherapeutic drug for pancreatic adenocarcinoma, supporting the development of an anti-cancer therapy based on UCP2 inhibition associated to standard chemotherapy. Our results demonstrate for the first time that UCP2 plays a role in autophagy regulation bringing new insights into mitochondrial uncoupling protein field.

1. Introduction

The uncoupling proteins (UCPs) belong to the mitochondrial anion transporter superfamily located in the inner mitochondrial membrane [1]. In mammals, five different UCP homologues have been described, UCP 1–5, which have different levels of identity and different tissue distribution [2–4]. Several studies have shown that the antioxidant UCP2 is broadly over-expressed in cancer cells [5,6], supporting this feature as an adaptive mechanism developed by tumors to maintain homeostasis of reactive oxygen species (ROS) [6,7]. The "uncoupling to survive" hypothesis conceives that a portion of the mitochondrial proton gradient used to drive ATP synthesis is "leaked" back into the matrix through UCP2 to render the electron flow through the respiratory complexes more efficient and to decrease mitochondrial superoxide emission [1,8]. Negre-Salvayre et al. first suggested a role for the uncoupling proteins in curtailing mitochondrial ROS production demonstrating that inhibition of UCP2 with GDP resulted in a sharp rise in H_2O_2 [9]. This evidence was later supported by our group among others demonstrating that UCP2 inhibition by siRNA or by the specific inhibitor genipin increases mitochondrial superoxide ion production in cancer cells [10], while UCP2 over-expression diminishes ROS production [11]. In addition, it was demonstrated that UCP2 plays a key role in the acquisition of drug-resistant cancer phenotypes protecting cells against the ROS generating properties of chemotherapeutics [10,12,13].

Autophagy (or self-eating) is a lysosome-mediated degradation process for non-essential or damaged cellular constituents. It is a multi-step process, involving the formation of double-membrane vesicles known as autophagosomes. Elongation of the autophagosomal membrane entails conjugation of MAP1-light chain 3 (LC3) protein to phosphatidylethanolamine to form a lipidated type of LC3 (LC3-II) [14], which is often used as a marker of autophagy. Autophagosomes mature and fuse with lysosomes to degrade their contents in the acidic environment mediated by acidic hydrolases. Physiologically, autophagy has the role to preserve the balance between organelle biogenesis, protein synthesis and their clearance. More recently, it has been shown that autophagy is an important mediator of pathological responses and is engaged in cross-talk with ROS in cell signaling and protein damage [15].

Besides its conventional metabolic role, the glycolytic enzyme glyceraldehyde 3-phosphate dehydrogenase (GAPDH) participates in diverse cellular functions, including autophagy [16]. An important level of regulation is the translocation of the enzyme to the nucleus, which can be triggered in response to oxidative stress [17]. Recently, it has been demonstrated that, upon nuclear translocation, GAPDH

* Corresponding author at: Dept. of Life and Reproduction Sciences, Section of Biochemistry, University of Verona, Strada Le Grazie 8, 37134 Verona, Italy. Tel.: +39 045 8027281; fax: +39 045 8027170.
E-mail address: massimo.donadelli@univr.it (M. Donadelli).

0167-4889/$ – see front matter © 2012 Elsevier B.V. All rights reserved.
http://dx.doi.org/10.1016/j.bbamcr.2012.10.028

contributes to cell death [18], autophagy protein Atg12 up-regulation and autophagy stimulation [19].

In the present study, we have investigated the regulation of autophagy in response to over-expression or inhibition of UCP2 and its role in pancreatic adenocarcinoma cell proliferation.

2. Materials and methods

2.1. Chemicals

Gemcitabine (2′,2′-difluoro-2′-deoxycytidine; Jemta; GEM) was provided by Sandoz Italia and was solubilized in sterile water. Genipin (methyl-2-hydroxy-9-hydroxymethyl-3-oxabicyclonona-4,8-diene-5-carboxylate) was obtained from Sigma (Milan, Italy), solubilized in DMSO and stored at −80 °C until use. *N*-acetyl-L-cysteine (NAC), chloroquine diphosphate (CQ), and 3-methyladenine (3-MA) were obtained from Sigma.

2.2. Cell culture

Human pancreatic adenocarcinoma cell lines PaCa44, PaCa3, and Panc1 were grown in RPMI 1640 supplemented with 2 mM glutamine (Life Technologies, Milan, Italy), 10% FBS, and 50 μg/ml gentamicin sulfate (BioWhittaker, Lonza, Bergamo, Italy). All cell lines were incubated at 37 °C with 5% CO_2.

2.3. Cell proliferation assay

Cells were seeded in 96-well plates (5×10^3 cells/well), 24 h later treated with various compounds and further incubated for the indicated times (see legends to figures). At the end of the treatments, cells were stained with a Crystal Violet solution (Sigma, Milan, Italy). The dye was solubilized in PBS containing 1% SDS and measured photometrically (A595nm) to determine cell growth. Three independent experiments were performed for each assay condition.

2.4. Over-expression and silencing of UCP2

UCP2 over-expression experiments were performed using a pCMV expression vector containing the human cDNA of UCP2 (OriGene Technologies, Rockville, MD) using TransIT-LT1 transfection reagent (Mirus, Tema Ricerca, Bologna, Italy). Cells transfected with the empty pCMV vector were used as a negative control (mock). Cells were incubated for 72 h to evaluate the effect of UCP2 over-expression on autophagosome formation.

UCP2 silencing experiments were carried out with a specific small interfering (si) (5′-GCUAAAGUCCGGUUACAGATT-3′) RNA targeting UCP2 mRNA and a non-targeting (NT) siRNA (5′-CAGUCGCGUUU GCGACUGG-3′) purchased by Ambion Life Technologies (Monza MB, Italy). Cells were transfected with siRNAs at a final concentration of 200 nM using Transfectin for 72 h (Biorad, Milan, Italy).

Transfection efficiency of PaCa44 cells was about 40% as previously assessed by cytofluorimetric analysis using a pGFP plasmid vector.

2.5. Analysis of ROS

The non-fluorescent diacetylated 2′,7′-dichlorofluorescein (DCF-DA) probe (Sigma), which becomes highly fluorescent upon oxidation, was used to evaluate intracellular ROS production. Briefly, cells were plated in 96-well plates (5×10^3 cells/well) and, 24 h later, treated with various compounds, as indicated in the legends to figures. Then, cells were incubated with 10 μM DCF-DA for 15 min at 37 °C, and the DCF fluorescence was measured by using a multimode plate reader (Ex 485 nm and Em 535 nm). The values were normalized on cell proliferation by Crystal Violet assay. Three independent experiments were performed for each assay condition.

2.6. Immunoblot analysis

To analyze GAPDH distribution nuclear and cytoplasmic protein extracts were obtained with Nuclear Extract Kit (Active Motif), electrophoresed through a 12% SDS-polyacrylamide gel, and electroblotted onto PVDF membranes (Millipore, Milan, Italy). To analyze LC3 isoforms (LC3-I and LC3-II) and UCP2 whole cell protein extracts were obtained with RIPA Buffer (50 mM Tris–HCl pH 7.5, 150 mM NaCl, 1% Igepal CA-630, 0.5% Na-Doc, 0.1% SDS, 1 mM Na_3VO_4, 1 mM NaF, 2.5 mM EDTA, 1 mM PMSF, and 1× protease inhibitor cocktail) followed by incubation on ice for 30 min. The lysate was centrifuged at 500 ×*g* for 10 min at 4 °C and the supernatant was electrophoresed through a 18% SDS-polyacrylamide gel and electroblotted onto PVDF membranes (Millipore, Milan, Italy). Membranes were then incubated with blocking solution [5% low-fat milk in TBST (100 mM Tris pH 7.5, 0.9% NaCl, 0.1% Tween 20)] for 1 h at room temperature and probed overnight at 4 °C with a rabbit monoclonal anti-GAPDH (1:1000 in blocking solution) (Cell Signaling), rabbit monoclonal anti-LC3 (1:1000) (Cell Signaling), or goat polyclonal anti-UCP2 (1:1000) (Abnova) antibodies. Horseradish peroxidase conjugated anti-rabbit IgG (1:8000) (Upstate Biotechnology, Milan, Italy) or anti-goat IgG (1:1000) (Santa Cruz Biotechnology) were used to detect specific proteins. Immunodetection was carried out using chemiluminescent substrates (Amersham Pharmacia Biotech, Milan, Italy) and recorded using a HyperfilmECL (Amersham Pharmacia Biotech). The bands were scanned as digital peaks and the areas of the peaks were calculated in arbitrary units using the public domain NIH Image software (http://rsb.info.nih.gov/nih-image/). The value of Ponceau S dye was used as a normalizing factor.

2.7. Immunofluorescence analysis

Cells (1.6×10^4) were grown on coverslips and treated with various compounds at the indicated concentrations for 16 h. Cells were permeabilized with PBS solution containing 3% BSA and 0.3% Triton X-100 at RT for 15 min and incubated with rabbit GAPDH-antibody (1:100) at RT for 90 min and then incubated with Alexa Fluor 488 anti-rabbit IgG antibody (1:500) at RT for 60 min. To assess nuclear morphology, cells were incubated with Hoechst at RT for 2 min. Fluorescence was visualized using excitation/emission wavelengths of 488/520 nm (green) and 350/460 nm (blue) for GAPDH and Hoechst, respectively. Cells were examined using TCS-SP5 Leica confocal microscope at 40× magnification.

2.8. Autophagosome formation assay

To quantify the induction of autophagy, cells were incubated with the fluorescent probe monodansylcadaverine (MDC; Sigma, Milan, Italy). MDC is a selective marker for acidic vesicular organelles (AVOs), such as autophagic vacuoles and especially autolysosomes. Briefly, cells were seeded in 96-well plates (5×10^3 cells/well) and treated with the various compounds as indicated in the legend. At the end of the treatments, cells were incubated in culture medium with 50 μM MDC at 37 °C for 15 min. After incubation, cells were washed with Hanks buffer (20 mM Hepes pH 7.2, 10 mM glucose, 118 mM NaCl, 4.6 mM KCl, and 1 mM $CaCl_2$) and fluorescence was measured by using a multimode plate reader (Ex 340 nm and Em 535 nm) (GENios Pro, Tecan, Milan, Italy). The values were normalized on cell proliferation by Crystal Violet assay. Three independent experiments were performed for each assay condition.

2.9. Apoptosis assay

Cells were seeded in 96-well plates (5×10^3 cells/well) and, the day after, treated with the various compounds at the indicated concentrations for 24 h. At the end of the treatment, cells were fixed

with 2% paraformaldehyde in PBS at room temperature for 30 min, then washed twice with PBS and stained with annexinV/FITC (Bender MedSystem, Milan, Italy) in binding buffer (10 mM HEPES/NaOH pH 7.4, 140 mM NaOH, and 2.5 mM $CaCl_2$) for 10 min at room temperature in the dark. Finally, cells were washed with binding buffer solution and fluorescence was measured by using a multimode plate reader (Ex 485 nm and Em 535 nm) (GENios Pro, Tecan, Milan, Italy). The values were normalized on cell proliferation by Crystal Violet assay. Three independent experiments were performed for each assay condition.

2.10. RNA extraction and qPCR

Total RNA was extracted from 10^6 cells using TRIzol Reagent (Life Technologies, Milan, Italy), and 1 μg of RNA was reverse transcribed using first-strand cDNA synthesis. Real-time quantification was performed in triplicate samples by SYBR Green detection chemistry with Power SYBR Green PCR Master Mix (Applied Biosystems) on a 7000 Sequence Detection System. The primers used were: Hs_UCP2_1_SG QuantiTect Primer Assay for the UCP2 gene and Hs_RRN18S_1_SG QuantiTect Primer Assay (Qiagen, Milan, Italy) for 18S rRNA. The amplification conditions consisted in an initial step of 15 min at 95 °C to activate HotStarTaq DNA polymerase and 45 cycles of denaturation at 94 °C for 15 s, annealing at 55 °C for 30 s, and extension at 72 °C for 30 s. Three independent experiments were performed for each assay condition.

2.11. Statistical analysis

ANOVA (post hoc Bonferroni) analysis was performed by GraphPad Prism 5 software. p values <0.05, 0.01, or 0.001 were indicated as (*), (**), or (*** or ###), respectively.

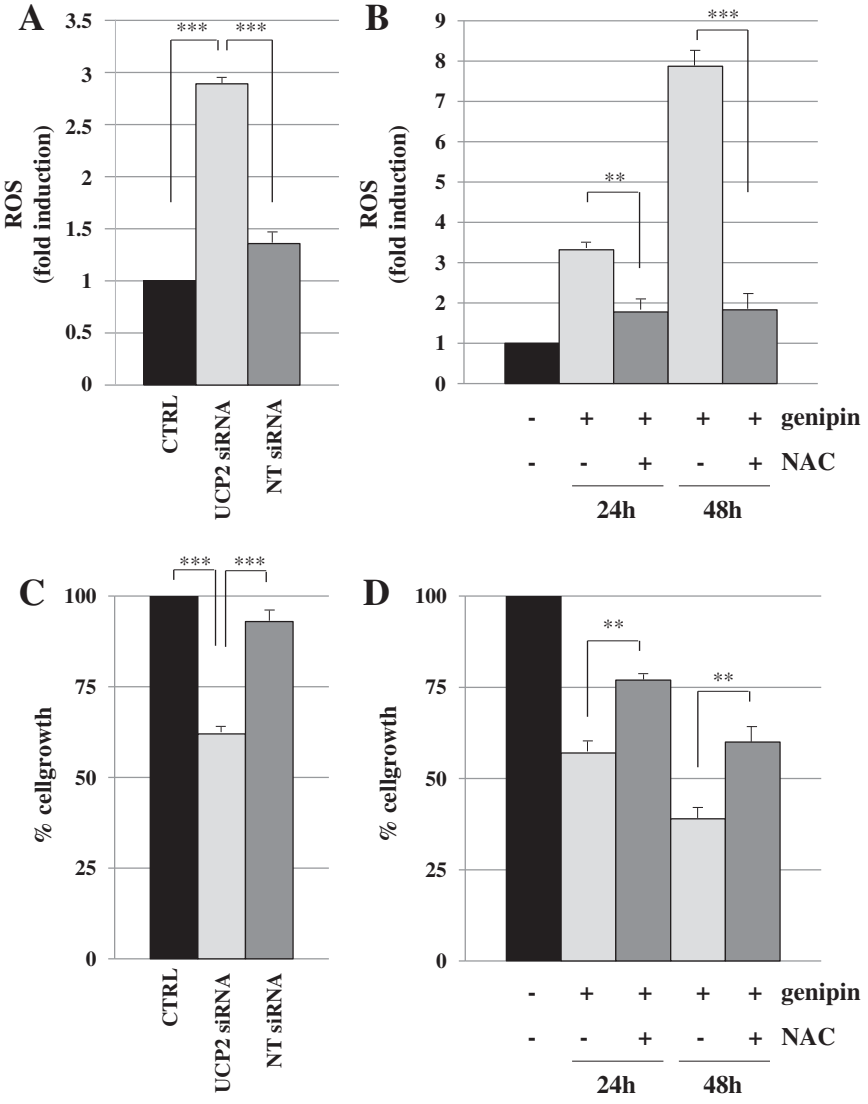

Fig. 1. Effect of UCP2 inhibition on ROS production and cell growth. (A) PaCa44 cells were seeded in 96-well plates, incubated overnight, and transfected with 200 nM UCP2 siRNA or NT siRNA for 72 h. The DCF fluorescence intensity, corresponding to the level of ROS production, was measured by a multimode plate reader. Statistical analysis: (***) $p<0.001$ UCP2 siRNA vs. CTRL or NT siRNA. (B) PaCa44 cells were seeded in 96-well plates, incubated overnight, pre-treated with 10 mM NAC for 1 h and then treated with 250 μM genipin for further 24 or 48 h. The DCF fluorescence intensity, corresponding to the level of ROS production, was measured by a multimode plate reader. Statistical analysis: (**) $p<0.01$ genipin vs. genipin + NAC (24 h); (***) $p<0.001$ genipin vs. genipin + NAC (48 h). (C) PaCa44 cells were seeded in 96-well plates, incubated overnight, and transfected with 200 nM UCP2 siRNA or NT siRNA for 72 h. Cell proliferation was determined using the Crystal Violet colorimetric assay. Statistical analysis: (***) $p<0.001$ UCP2 siRNA vs. CTRL or NT siRNA. (D) PaCa44 cells were seeded in 96-well plates, incubated overnight, pre-treated with 10 mM NAC for 1 h and then treated with 250 μM genipin for further 24 or 48 h. Cell proliferation was determined using the Crystal Violet colorimetric assay. Statistical analysis: (**) $p<0.01$ genipin vs. genipin + NAC. For all experiments, values are the means (± SD) of three independent experiments each performed in triplicate.

3. Results

3.1. UCP2 inhibition induces ROS-mediated pancreatic adenocarcinoma cell growth inhibition

To evaluate the effect of UCP2 inhibition on intracellular ROS production, we performed ROS assays on PaCa44 adenocarcinoma cells treated with UCP2 siRNA or the specific UCP2 inhibitor genipin. Fig. 1A and B shows that ROS production was enhanced by both UCP2 silencing and genipin and that genipin-mediated ROS enhancement was almost completely hampered by the radical scavenger NAC. Cell proliferation assay demonstrated that UCP2 siRNA (Fig. 1C) or genipin (Fig. 1D) inhibited PaCa44 cell growth and that, consistent with Fig. 1B, genipin-mediated effect was significantly reduced by NAC at both 24 and 48 h (Fig. 1D). UCP2 mRNA and protein levels after UCP2 siRNA or NT siRNA transfections were analyzed using qRT-PCR (Supplementary Fig. 1A) and Western blot (Supplementary Fig. 1C).

3.2. UCP2 inhibition stimulates ROS-dependent nuclear translocation of GAPDH

Since GAPDH is a redox-sensitive enzyme and oxidative stress can stimulate its nuclear translocation, we analyzed cellular distribution of GAPDH after treatment with genipin and/or NAC for 16 h. Fig. 2A shows that GAPDH translocated into the nucleus of the cells after UCP2 inhibition by genipin and that this effect was hampered by NAC. To confirm this result, we performed Western blot analyses using nuclear or cytoplasmic protein extracts. Fig. 2B and C shows that genipin strongly increased GAPDH expression level in the nuclear fraction of the cells and that this event was totally inhibited by NAC.

3.3. UCP2 inhibition induces ROS-dependent autophagy

Since GAPDH nuclear translocation is a strictly autophagy-related event, we performed autophagosome formation assay and Western blot analysis of LC3 isoforms after modulation of UCP2. We demonstrate that UCP2 over-expression reduced both endogenous ROS (Fig. 3A) and constitutive autophagosome formation of about 40%, while UCP2 silencing strongly enhanced autophagy (Fig. 3B). UCP2 mRNA and protein levels after pCMV-UCP2 or empty vector transfections were analyzed using qRT-PCR (Supplementary Fig. 1B) and Western blot (Supplementary Fig. 1C). Fig. 3C and D show that the induction of autophagosomes and of LC3-II/LC3-I ratio expression level by genipin was inhibited by NAC, demonstrating that oxidative stress is required to stimulate autophagy by UCP2 inhibition. To further investigate autophagy regulation by UCP2, we extended autophagy assays to two additional pancreatic adenocarcinoma cell lines (Panc1 and PaCa3). Data reported in Supplementary Fig. 2A and B show, respectively, that autophagosomes formation is induced by UCP2 siRNA in a concentration-dependent manner in Panc1 cells and that the expression level of LC3-II isoform was enhanced by genipin in both PaCa3 and Panc1 cell lines. Fig. 3E shows the regulation of ROS,

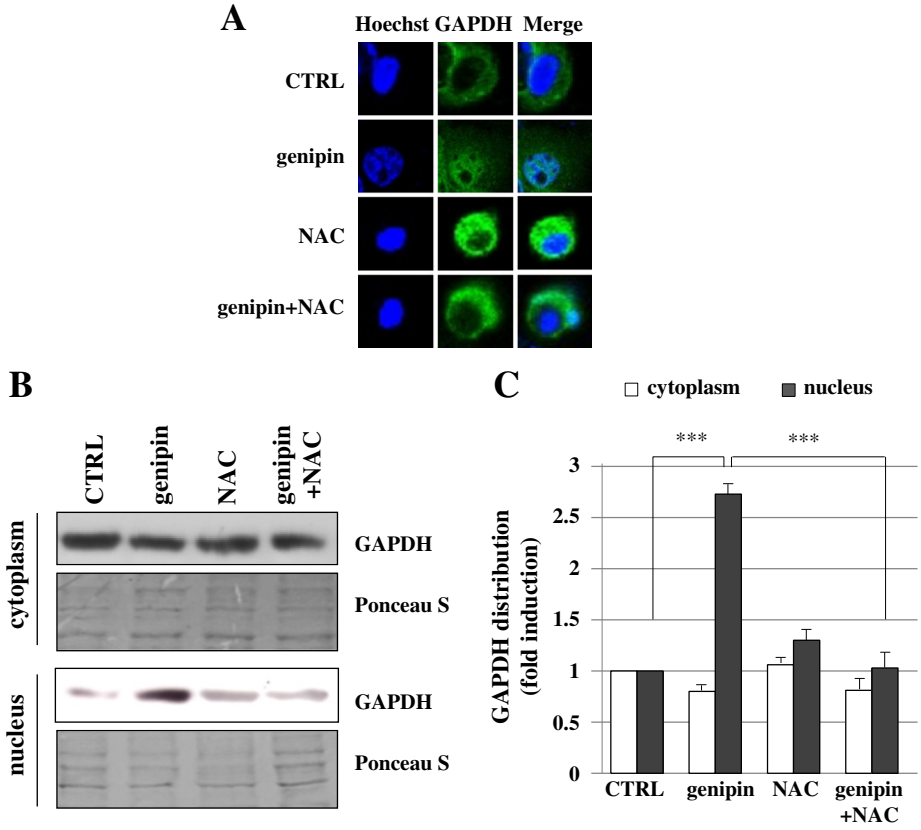

Fig. 2. Effect of UCP2 inhibition on cellular distribution of GAPDH. (A) PaCa44 cells were pre-treated with 10 mM NAC for 1 h and/or treated with 250 μM genipin for 16 h. GAPDH immunoreactivity (green) appeared within cell nuclei (blue labeled with Hoechst) only in cells exposed to genipin. The results shown are representative of three independent experiments. (B) Western blot analysis of GAPDH expression levels in PaCa44 cells pre-treated with 10 mM NAC for 1 h and/or treated with 250 μM genipin for 16 h. Nuclear and cytoplasmic protein extracts were obtained as described in Material and methods. Ponceau S staining was used as control loading. (C) Quantitative evaluation of GAPDH expression levels in the nucleus and cytoplasm of the cells. The bands of Western blot analyses were scanned as digital peaks and the areas of the peaks were calculated in arbitrary units. The value of Ponceau S dye was used as a normalizing factor. Values are the means (±SD) of three independent experiments. Statistical analysis: (***) $p<0.001$ genipin vs. CTRL or genipin + NAC (for nuclear localization).

autophagy, and cell growth after treatment of PaCa44 cells with increasing concentrations of genipin for 24 h. The trends of ROS induction and of autophagosomes formation were very similar and inversely correlated to cell growth, suggesting an antiproliferative role of ROS-dependent autophagy by UCP2 inhibition. Comparable results were obtained after PaCa44 cell treatment with increasing concentrations of genipin for 48 h (Supplementary Fig. 3). To exclude unspecific or side effects of genipin in cells [13], we evaluated cell growth, ROS, and autophagy in PaCa44 cells after a long exposure (6 days) to increasing concentrations of genipin. We observed that as low as 25 μM genipin was sufficient to inhibit PaCa44 cell proliferation and to induce ROS and autophagy (Supplementary Fig. 4).

3.4. Autophagy induced by UCP2 inhibition has an antiproliferative role

To further analyze the role of autophagy stimulation on cell proliferation and apoptosis by UCP2 inhibition, we treated PaCa44 cells with genipin and/or the autophagy inhibitors chloroquine (CQ) or

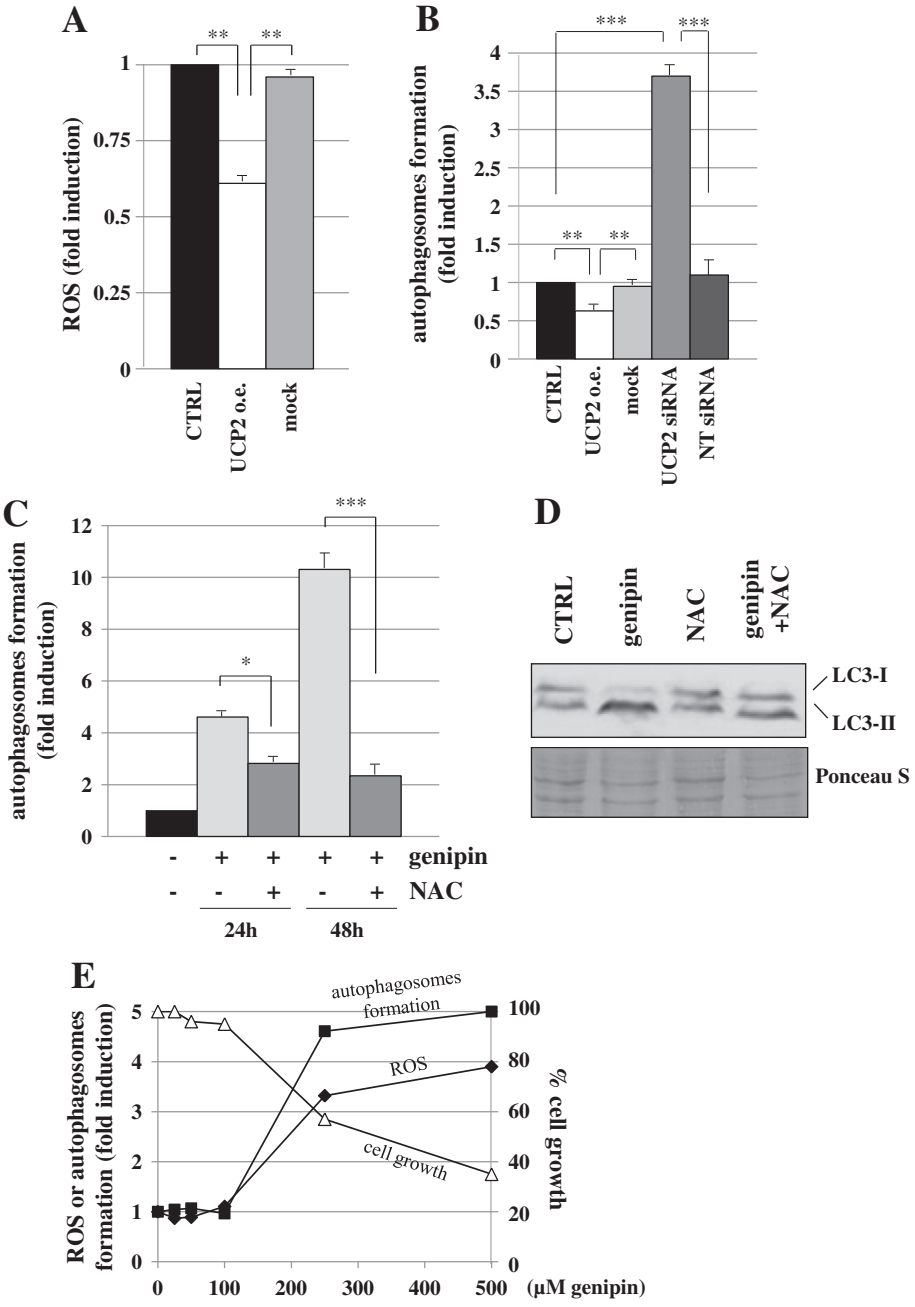

Fig. 3. Effect of UCP2 over-expression or inhibition on autophagy. (A) PaCa44 cells were seeded in 96-well plates, incubated overnight, and transfected with 200 ng/well pCMV-UCP2 or empty pCMV vector (mock) for 72 h. The DCF fluorescence intensity, corresponding to the level of ROS production, was measured by a multimode plate reader. Statistical analysis: (**) $p<0.01$ UCP2 o.e. vs. CTRL or mock. (B) PaCa44 cells were seeded in 96-well plates, incubated overnight, and transfected with 200 ng/well pCMV-UCP2 or empty pCMV vector (mock) for 72 h, or 200 nM UCP2 siRNA or NT siRNA for 72 h. Statistical analysis: (**) $p<0.01$ UCP2 o.e. vs. CTRL or mock; (***) $p<0.001$ UCP2 siRNA vs. CTRL or NT siRNA. (B) PaCa44 cells were seeded in 96-well plates, incubated overnight, pre-treated with 10 mM NAC for 1 h and then treated with 250 μM genipin for further 24 or 48 h. Statistical analysis: (*) $p<0.05$ genipin vs. genipin + NAC (24 h); (***) $p<0.001$ genipin vs. genipin + NAC (48 h). Autophagosome formation assay (A and B) was analyzed using the incorporation of monodansylcadaverine (MDC) probe. Values are the means (± SD) of three independent experiments each performed in triplicate. (C) PaCa44 cells were seeded in 100-mm diameter culture dishes, incubated overnight, pre-treated with 10 mM NAC for 1 h and then treated with 250 μM genipin for 24 h. Whole-cell extracts were used for Western blot analysis of the autophagic marker LC3. (D) Quantitative evaluations of autophagosome formation, ROS production, and cell growth of PaCa44 cells treated with increasing concentrations of genipin for 24 h.

3-methyladenine (3-MA), or the radical scavenger NAC. Fig. 4A and B shows that both UCP2 siRNA and genipin induced pancreatic adenocarcinoma apoptotic cell death. In addition, Fig. 4B shows that genipin-mediated apoptosis was strongly reduced in the presence of CQ, 3-MA, or NAC. Consistently, Fig. 4C reports that PaCa44 cell growth inhibition by genipin was significantly attenuated by autophagy inhibitors. Altogether, these data indicate that ROS-dependent autophagy induced by UCP2 inhibition in pancreatic adenocarcinoma cells is an event that favors apoptotic cell death.

3.5. Genipin/gemcitabine combined treatment strongly enhances autophagy

To evaluate whether UCP2 inhibition can enhance autophagy induced by gemcitabine, the standard chemotherapeutic drug for pancreatic adenocarcinoma, we performed autophagosome formation assay in PaCa44 cells treated with genipin and/or gemcitabine for 24 and 48 h. Fig. 5 shows that genipin induced autophagy at a higher extent than gemcitabine and that their combination significantly potentiates autophagy triggered by single treatments at both 24 and 48 h treatments. These data strongly suggest that the enhancement of autophagy induction by the combined treatment genipin/gemcitabine could have a role in their antiproliferative synergism (described in [10]).

4. Discussion

In the present study, we clearly elucidate for the first time the role of UCP2-mediated mitochondrial uncoupling on autophagy regulation in cancer cells. It is well known that UCP2 is an antioxidant mitochondrial protein whose inhibition induces oxidative stress favoring the formation of mitochondrial superoxide ions [6]. Here, we show that ROS induction is required for nuclear translocation of the glycolytic enzyme GAPDH and for autophagic cell death triggered by UCP2 inhibition. Our data are in agreement with the observations of Watanabe and colleagues who demonstrated that suppression of another member of the UCP superfamily (UCP3) enhances the expression of the autophagic phenotype in epiphyseal chondrocytes rendering the cells more susceptible to apoptogens [20]. Recently, it has been demonstrated that

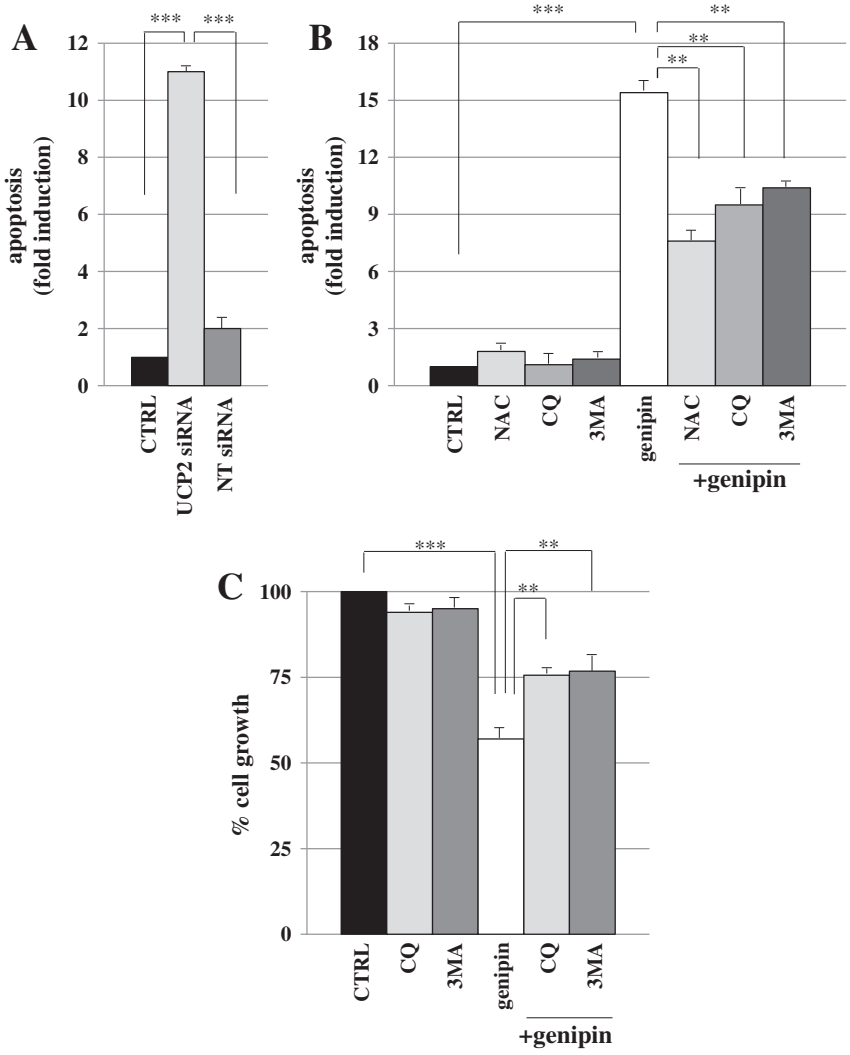

Fig. 4. Effect of autophagy inhibitors on apoptotic cell death by UCP2 inhibition. (A) Cells were seeded in 96-well plates, incubated overnight, and transfected with 200 nM UCP2 siRNA or NT siRNA for 72 h. Statistical analysis: (***) $p<0.001$ UCP2 siRNA vs. CTRL or NT siRNA. (B) PaCa44 cells were seeded in 96-well plates, incubated overnight, pre-treated with 10 mM NAC, 5 μM CQ, or 2.5 mM 3-MA for 1 h and then treated with 250 μM genipin for further 24 h. Statistical analysis: (**) $p<0.01$ genipin vs. genipin + NAC, genipin + CQ, or genipin + 3MA; (***) $p<0.001$ genipin vs. CTRL. Apoptosis (A and B) was analyzed using the annexinV binding assay. Values are the means (±SD) of three independent experiments each performed in triplicate. (C) PaCa44 cells were seeded in 96-well plates, incubated overnight, pre-treated 5 μM CQ or 2.5 mM 3-MA for 1 h and then treated with 250 μM genipin for further 24 h. Cell proliferation was determined using the Crystal Violet colorimetric assay. Values are the means (±SD) of three independent experiments each performed in triplicate. Statistical analysis: (**) $p<0.01$ genipin vs. genipin + CQ, or genipin + 3MA; (***) $p<0.001$ genipin vs. CTRL.

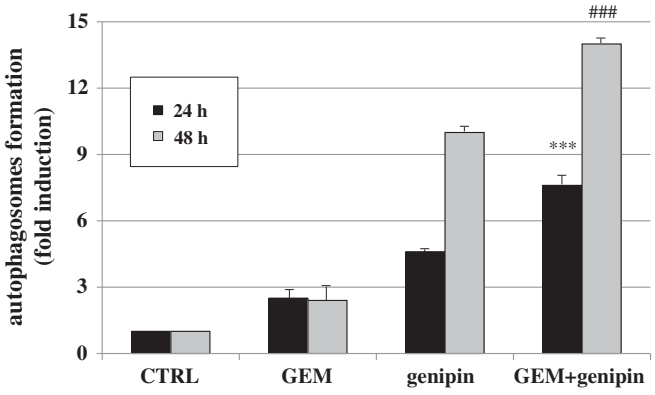

Fig. 5. Effect of genipin and/or gemcitabine on autophagy. PaCa44 cells were seeded in 96-well plates, incubated overnight, and treated with 500 nM GEM and/or 250 μM genipin for 24 and 48 h. Autophagosome formation assays were performed using the incorporation of monodansylcadaverine (MDC) probe. Values are the means (±SD) of three independent experiments each performed in triplicate. Statistical analysis: (***) $p<0.001$ GEM + genipin vs. GEM or genipin (24 h); (###) $p<0.001$ GEM + genipin vs. GEM or genipin (48 h).

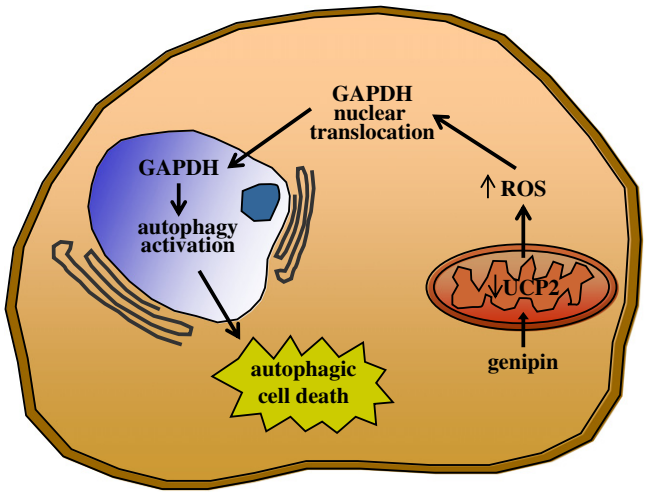

Fig. 6. Model of autophagy induction by genipin. The molecular mechanisms identified in this study are shown. See text for further details.

GAPDH is a key redox-sensitive protein, the activity of which is largely affected by covalent oxidative modifications at its highly reactive Cys^{152} residue that stimulate nuclear translocation of the enzyme and regulate the fate of the cell [16]. GAPDH translocation into the nuclei can be decoded as an extreme effort of the cell to maintain ROS production into tolerable levels. Indeed, studies in *Caenorhabditis elegans* indicated that redox regulation of GAPDH can counteract oxidative stress by repressing the glycolytic pathway and consequently rerouting the metabolic flux to maintain an optimal NADPH/$NADP^+$ ratio through the pentose phosphate pathway (PPP) [21]. Enzymes of the PPP are crucial for maintaining the cytoplasmic NADPH concentration, which provides the redox power for known antioxidant systems [22]. Accordingly, it is remarkable that under oxidative stress conditions the expression of a subset of glycolytic proteins is repressed, while the expression of a few enzymes involved in the PPP is induced [23]. Consistent with this finding, enhanced activity of the PPP has been observed in neonatal rat cardiomyocytes and in human epithelial cells after oxidative stress stimulation [24,25]. Intriguingly, Colell and colleagues indentified a novel role for GAPDH in autophagy induction demonstrating that its nuclear translocation participates in the up-regulation of the autophagy protein Atg12 and that enforced expression of Atg12 obviated the requirement for nuclear GAPDH [19].

Since AMPK is a positive regulator of autophagy during energetic crisis and a key enzyme involved in GAPDH nuclear translocation by direct phosphorylation [26], while mTOR is a known inhibitor of autophagy [27], we analyzed the active/phosphorylated form of AMPK and p70S6K, a direct target of mTOR signaling, following UCP2 inhibition by genipin. Surprisingly, we observed that genipin inhibited AMPK phosphorylation and induced p70S6K phosphorylation (data not shown), thus excluding the involvement of AMPK in nuclear translocation of GAPDH and autophagy stimulation by UCP2 inhibition. These observations further sustain the role of ROS in GAPDH nuclear translocation and autophagy, and suggest the absence of a catabolic autophagic mechanism driven by cellular energetic default. Although the identification of the molecular mechanisms at the basis of AMPK inhibition and mTOR activation needs further investigations, one may speculate that the regulations of these enzymes can be an extreme attempt of cancer cells to moderate an excessive and citotoxic autophagy stimulation. Indeed, it is well described that autophagy can act as a protective mechanism during a stressful episode helping cancer cells to maintain their survival in a setting of increased metabolic demands or hypoxic microenvironment, or, if prolonged, it can lead to cell death, named "autophagic cell death" [28,29]. In the present study, we demonstrate that autophagy induced by UCP2 inhibition encloses a cancer cell death feature. Indeed, the addition of the autophagy inhibitors CQ or 3-MA or the antioxidant NAC strongly reduced pancreatic adenocarcinoma apoptotic cell death preserving cell survival.

Furthermore, we show that UCP2 inhibition enhanced autophagy induced by gemcitabine, the standard chemotherapeutic drug for pancreatic cancer. Recently, our group demonstrated that gemcitabine is able to induce UCP2 mRNA and that targeted inhibition of UCP2 dramatically increases the sensitivity to gemcitabine of several cancer cell types in a ROS-dependent mechanism [10]. Altogether these observations, added to the previous demonstration that autophagy by gemcitabine is a cell death mechanism [30,31], suggest that UCP2 mRNA induction by gemcitabine is a protective mechanism of cancer cells involved in the attenuation of autophagy and that the enhanced autophagy induced by genipin/gemcitabine combined treatment has a role in their antiproliferative synergism (described in [10]). The major molecular events deduced from our data are reported in Fig. 6.

5. Conclusions

In the present study we have clearly demonstrated for the first time the involvement of UCP2 in the ROS-dependent autophagy regulation of cancer cells supporting the usage of UCP2 inhibitors in the anti-tumoral strategy for pancreatic adenocarcinoma and bringing new insights in the field of mitochondrial uncoupling proteins.

Supplementary data to this article can be found online at http://dx.doi.org/10.1016/j.bbamcr.2012.10.028.

Acknowledgements

This work was supported by Associazione Italiana Ricerca Cancro (AIRC), Milan, Italy; Fondazione CariPaRo, Padova, Italy; Ministero dell'Istruzione, dell'Università e della Ricerca (MIUR), Rome, Italy; and Progetti di Ricerca di Interesse Nazionale (PRIN, MIUR), Rome, Italy.

References

[1] R.J. Mailloux, M.E. Harper, Uncoupling proteins and the control of mitochondrial reactive oxygen species production, Free Radic. Biol. Med. 51 (2011) 1106–1115.
[2] S.H. Adams, G. Pan, X.X. Yu, Perspectives on the biology of uncoupling protein (UCP) homologues, Biochem. Soc. Trans. 29 (2001) 798–802.
[3] S. Dridi, O. Onagbesan, Q. Swennen, J. Buyse, E. Decuypere, M. Taouis, Gene expression, tissue distribution and potential physiological role of uncoupling protein in avian species, Comp. Biochem. Physiol. A Mol. Integr. Physiol. 139 (2004) 273–283.
[4] J.S. Kim-Han, L.L. Dugan, Mitochondrial uncoupling proteins in the central nervous system, Antioxid. Redox Signal. 7 (2005) 1173–1181.

[5] V. Ayyasamy, K.M. Owens, M.M. Desouki, P. Liang, A. Bakin, K. Thangaraj, D.J. Buchsbaum, A.F. LoBuglio, K.K. Singh, Cellular model of Warburg effect identifies tumor promoting function of UCP2 in breast cancer and its suppression by genipin, PLoS One 6 (2011) e24792.
[6] G. Baffy, Uncoupling protein-2 and cancer, Mitochondrion 10 (2010) 243–252.
[7] G. Baffy, Z. Derdak, S.C. Robson, Mitochondrial recoupling: a novel therapeutic strategy for cancer? Br. J. Cancer 105 (2011) 469–474.
[8] M.D. Brand, T.C. Esteves, Physiological functions of the mitochondrial uncoupling proteins UCP2 and UCP3, Cell Metab. 2 (2005) 85–93.
[9] A. Negre-Salvayre, C. Hirtz, G. Carrera, R. Cazenave, M. Troly, R. Salvayre, L. Penicaud, L. Casteilla, A role for uncoupling protein-2 as a regulator of mitochondrial hydrogen peroxide generation, FASEB J. 11 (1997) 809–815.
[10] E. Dalla Pozza, C. Fiorini, I. Dando, M. Menegazzi, A. Sgarbossa, C. Costanzo, M. Palmieri, M. Donadelli, Role of mitochondrial uncoupling protein 2 in cancer cell resistance to gemcitabine, Biochim. Biophys. Acta 1823 (2012) 1856–1863.
[11] K.U. Lee, I.K. Lee, J. Han, D.K. Song, Y.M. Kim, H.S. Song, H.S. Kim, W.J. Lee, E.H. Koh, K.H. Song, S.M. Han, M.S. Kim, I.S. Park, J.Y. Park, Effects of recombinant adenovirus-mediated uncoupling protein 2 overexpression on endothelial function and apoptosis, Circ. Res. 96 (2005) 1200–1207.
[12] Z. Derdak, N.M. Mark, G. Beldi, S.C. Robson, J.R. Wands, G. Baffy, The mitochondrial uncoupling protein-2 promotes chemoresistance in cancer cells, Cancer Res. 68 (2008) 2813–2819.
[13] R.J. Mailloux, C.N. Adjeitey, M.E. Harper, Genipin-induced inhibition of uncoupling protein-2 sensitizes drug-resistant cancer cells to cytotoxic agents, PLoS One 5 (2010) e13289.
[14] Y. Kabeya, N. Mizushima, A. Yamamoto, S. Oshitani-Okamoto, Y. Ohsumi, T. Yoshimori, LC3, GABARAP and GATE16 localize to autophagosomal membrane depending on form-II formation, J. Cell Sci. 117 (2004) 2805–2812.
[15] J. Lee, S. Giordano, J. Zhang, Autophagy, mitochondria and oxidative stress: cross-talk and redox signalling, Biochem. J. 441 (2012) 523–540.
[16] A. Colell, D.R. Green, J.E. Ricci, Novel roles for GAPDH in cell death and carcinogenesis, Cell Death Differ. 16 (2009) 1573–1581.
[17] Z. Dastoor, J.L. Dreyer, Potential role of nuclear translocation of glyceraldehyde-3-phosphate dehydrogenase in apoptosis and oxidative stress, J. Cell Sci. 114 (2001) 1643–1653.
[18] T.M. Leisner, C. Moran, S.P. Holly, L.V. Parise, CIB1 prevents nuclear GAPDH accumulation and non-apoptotic tumor cell death via AKT and ERK signaling, Oncogene (2012), http://dx.doi.org/10.1038/onc.2012.408.
[19] A. Colell, J.E. Ricci, S. Tait, S. Milasta, U. Maurer, L. Bouchier-Hayes, P. Fitzgerald, A. Guio-Carrion, N.J. Waterhouse, C.W. Li, B. Mari, P. Barbry, D.D. Newmeyer, H.M. Beere, D.R. Green, GAPDH and autophagy preserve survival after apoptotic cytochrome c release in the absence of caspase activation, Cell 129 (2007) 983–997.
[20] H. Watanabe, J. Bohensky, T. Freeman, V. Srinivas, I.M. Shapiro, Hypoxic induction of UCP3 in the growth plate: UCP3 suppresses chondrocyte autophagy, J. Cell. Physiol. 216 (2008) 419–425.
[21] M. Ralser, M.M. Wamelink, A. Kowald, B. Gerisch, G. Heeren, E.A. Struys, E. Klipp, C. Jakobs, M. Breitenbach, H. Lehrach, S. Krobitsch, Dynamic rerouting of the carbohydrate flux is key to counteracting oxidative stress, J. Biol. 6 (2007) 10.
[22] N. Pollak, C. Dolle, M. Ziegler, The power to reduce: pyridine nucleotides — small molecules with a multitude of functions, Biochem. J. 402 (2007) 205–218.
[23] C. Godon, G. Lagniel, J. Lee, J.M. Buhler, S. Kieffer, M. Perrot, H. Boucherie, M.B. Toledano, J. Labarre, The H2O2 stimulon in *Saccharomyces cerevisiae*, J. Biol. Chem. 273 (1998) 22480–22489.
[24] D.R. Janero, D. Hreniuk, H.M. Sharif, Hydroperoxide-induced oxidative stress impairs heart muscle cell carbohydrate metabolism, Am. J. Physiol. 266 (1994) C179–C188.
[25] C. Le Goffe, G. Vallette, L. Charrier, T. Candelon, C. Bou-Hanna, J.F. Bouhours, C.L. Laboisse, Metabolic control of resistance of human epithelial cells to H2O2 and NO stresses, Biochem. J. 364 (2002) 349–359.
[26] H.J. Kwon, J.H. Rhim, I.S. Jang, G.E. Kim, S.C. Park, E.J. Yeo, Activation of AMP-activated protein kinase stimulates the nuclear localization of glyceraldehyde 3-phosphate dehydrogenase in human diploid fibroblasts, Exp. Mol. Med. 42 (2010) 254–269.
[27] Y. Li, J. Zhang, X. Chen, T. Liu, W. He, Y. Chen, X. Zeng, Molecular machinery of autophagy and its implication in cancer, Am. J. Med. Sci. 343 (2012) 155–161.
[28] I. Amelio, G. Melino, R.A. Knight, Cell death pathology: cross-talk with autophagy and its clinical implications, Biochem. Biophys. Res. Commun. 414 (2011) 277–281.
[29] M. Donadelli, I. Dando, T. Zaniboni, C. Costanzo, E. Dalla Pozza, M.T. Scupoli, A. Scarpa, S. Zappavigna, M. Marra, A. Abbruzzese, M. Bifulco, M. Caraglia, M. Palmieri, Gemcitabine/cannabinoid combination triggers autophagy in pancreatic cancer cells through a ROS-mediated mechanism, Cell Death Dis. 2 (2011) e152.
[30] H. Mukubou, T. Tsujimura, R. Sasaki, Y. Ku, The role of autophagy in the treatment of pancreatic cancer with gemcitabine and ionizing radiation, Int. J. Oncol. 37 (2010) 821–828.
[31] R. Pardo, A. Lo Re, C. Archange, A. Ropolo, D.L. Papademetrio, C.D. Gonzalez, E.M. Alvarez, J.L. Iovanna, M.I. Vaccaro, Gemcitabine induces the VMP1-mediated autophagy pathway to promote apoptotic death in human pancreatic cancer cells, Pancreatology 10 (2010) 19–26.